

Nonstationary hemodynamics modelling in a cerebral aneurysm of a blood vessel

A. A. Yanchenko^{*}, A. A. Cherevko^{*†}, A. P. Chupakhin^{*†}, A. L. Krivoshapkin[‡],
and K. Yu. Orlov[‡]

Abstract — Computer simulation is carried out for unsteady hemodynamics in a cerebral aneurysm of a blood vessel. Using the data of a real patient obtained in medical examination and during surgery, we reconstruct the 3D geometry of the anomaly, calculate hydrodynamic parameters of blood flow (flow velocity, streamline distribution, pressure, shear stress on walls, energy flux) and the deformation and stresses of the vessel walls. The calculations were performed for the following three cases: in the presence of an aneurysm, immediately after stent deployment changing the geometry of the vessel, and one year after the surgery. It is shown what changes of hydrodynamic and mechanical quantities characterize a successful surgery.

Keywords: Hemodynamics, cerebral aneurysm, stenting.

The vascular system of the brain is highly susceptible to anomalies and pathologies due to peculiar intensity of its work in comparison with other organs. Cerebral arterial aneurysms are the most common anomalies. They are a pathological local expansion of a vessel caused by inflation of one layers of its wall, namely, intima, which is the most subtle and least durable. This violates the geometry of the vessel and normal blood flow in it. Since the aneurysm dome is thinner than the vessel wall, in most cases there is a risk of rupture just at this place, which leads to hemorrhage. The aneurysm treatment scenario depends on many factors.

The hemodynamics in a neighbourhood of an aneurysm is intensively studied now. The influence of the geometry of the stent and vascular intracranial aneurysms were considered in [3, 5]. A simulation of flow-redirecting stent deployment was performed in [15]. An evaluation of stresses on the wall of an abdominal aortic aneurysms was done in [10]. The simulation results for the flow with an installed stent in the abdominal aorta was described in [12]. Mechanical properties of stents were studied in [13].

Currently, the outcome of the surgery depends on the skill of a particular surgeon. The medical aspects of the problem were described in details in [7]. This paper

^{*}Novosibirsk State University, Novosibirsk 630090, Russia

[†]Lavrent'ev Institute of Hydrodynamics, Siberian Branch of the RAS, Novosibirsk 630090, Russia

[‡]E. N. Meshalkin Research Institute of Blood Circulation Pathology, Novosibirsk 630055, Russia

The work was supported by the Siberian Branch of the RAS (Integration Project No. 44), the Program No. 2.13.4 of the Department of power engineering, machine building, mechanics and control processes of the RAS, and the Russian Foundation for Basic Research (14–01–00036).

is aimed to application of the methods of mathematical modelling to this complicated area.

Stents are often used for the surgery of arterial aneurysms without neck or aneurysms located in the bifurcation (branching) of vessels. There are many designs of stents used for different purposes. Any stent is a delicate, generally cylindrical, metal, or plastic construction. The stent is delivered to the place with an intravascular instrument and then is spread inside with a special removable bulb which increases its diameter and presses it into the vessel wall. The design of the stent ensures the preservation of its straightened configuration. In this paper we consider coarse elastic stents which practically do not block the lumen of the vessel but, due to their elasticity, gradually correct pathological bends of vessels. The stenting was not aimed at strengthening the walls in the zone of aneurysm and hence stents are positioned so that they do not touch initially the dome of the aneurysm. Mechanical properties of vessel walls in the zone of strengthening with stents could not be determined *in vivo*, at the same time, zones of maximal strains and stresses are located on the dome of the aneurysm or near it, i.e., in the areas where the interaction of the vessel wall and the stent does not occur. In this connection, calculations of the stress–strain state did not take into account the strengthening of vessel walls by a stent.

In this paper we study an unstationary mathematical model of hemodynamics in an aneurysm surgery, and the stress–strain state of walls is calculated subject to differences in their mechanical properties in the zone of aneurysm. Numerical calculations were performed with the use of ANSYS/Flucht and ANSYS/Mechanical packages in the information and computing complex of the Novosibirsk State University.

We simulate the actual surgery carried out by neurosurgeons of the Acad. E. N. Meshalkin Research Institute of Blood Circulation Pathology. The geometry of vessels is determined from the data of X-ray tomography. Elastic properties of vessel walls are taken from [22]. In order to specify boundary conditions, we take the values of the pressure and velocity of blood flow measured in cerebral vessels during the surgery. These measurements were taken near the pathology with the intravascular ComboWire sensor of the Volcano ComboMap instrument [8]. Three geometric configurations are considered, namely, before the surgery, immediately after the surgery, and checkup one (one year later).

Modelling of such complex and multifactor objects always poses a problem of optimization of the complexity of the model for choosing the model as simple as possible, but taking into account ‘significant’ factors. In this paper we describe the blood flow by unstationary Navier–Stokes equations for a viscous, incompressible, Newtonian fluid. The behaviour of vessel walls is described by equations of the linear theory of elasticity. The results of calculations indicate that the proposed model describes the change of hydrodynamic and mechanical parameters of the flow and vessel qualitatively and correctly and thus can be used in pre-surgery simulation, which is an important and promising approach of modern medicine.

The authors had considered the same surgery previously [29]. The description of

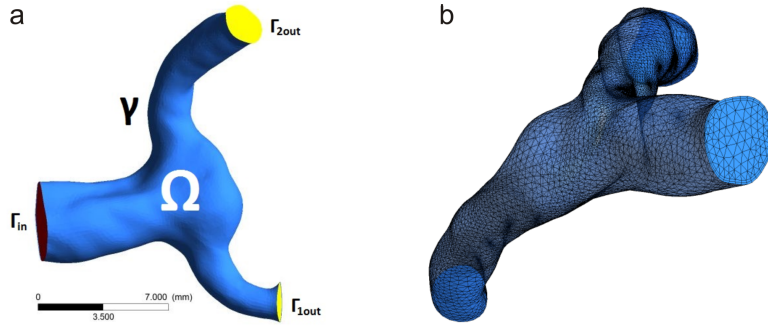


Figure 1. Calculation domain (a); calculation grid (b).

blood flow used stationary Navier–Stokes equations for a viscous, incompressible, Newtonian fluid, and the behaviour of vessel walls was described by equations of the linear theory of elasticity without separating the zone of aneurysm. It was shown that the flow velocity and shear stress on the wall were reduced after the surgery, the maximum of stresses was on the inner side of the aneurysm (before the surgery it was on the wall of the incoming flow, after the surgery it was at the point of flow stagnation). The points of maximal displacements and stresses were different both before and after the surgery.

1. Mathematical model

The blood flow is described by the Navier–Stokes equations for a three-dimensional unstationary flow of an incompressible, viscous, Newtonian fluid:

$$\begin{cases} \operatorname{div} \mathbf{v} = 0 \\ \mathbf{v}_t + (\mathbf{v} \cdot \nabla) \mathbf{v} + \nabla p = \nu \Delta \mathbf{v} \end{cases} \quad \text{in } \Omega. \quad (1.1)$$

Here, \mathbf{v} is the velocity, p is the pressure, ν is the coefficient of kinematic viscosity, Ω is the inner volume of the calculation domain including the configuration of vessels in the form of T-joint and the aneurysm located in the place of bifurcation. By $\gamma = \partial\Omega$ we denote the boundary of the vessel wall, Γ_{in} is the cross-section of the parent vessel of the tee, $\Gamma_{1\text{out}}$, $\Gamma_{2\text{out}}$ are the sections of subsidiary receptacles (outlets of the tee). In the solution of the hydrodynamic problem the vessel walls are assumed to be motionless.

For Navier–Stokes equations (1.1) we specify adhesion conditions on the walls of the vessel, i.e., $\mathbf{v} = 0$ on γ . On the normal section of the inlet vessel Γ_{in} we specify the variable velocity v_{real} , the conditions on output sections of the subsidiary vessels $\Gamma_{1\text{out}}$, $\Gamma_{2\text{out}}$ use variable pressure values p_{real}^1 and p_{real}^2 .

A similar formulation of boundary conditions is recommended in the manual for the ANSYS/Fluent package [1,2] and is widely used in computational practice (see, e.g., survey [4]). The well-definiteness of the streaming problem for the Navier–Stokes equations with such boundary conditions is a traditional assumption in such

numerical experiments and is justified by appropriate results of numerous calculations. Various formulations of boundary conditions on inflow/outflow regions are considered now for the Navier-Stokes equations for a viscous incompressible fluid in the streaming problem. Along with specification of velocity vectors, it is possible to specify the pressure and one velocity component on these regions so that the velocity vector is perpendicular to the inflow/outflow boundary [9, 25]. For the hydroelastic streaming problem one can specify the head (total pressure) and the equality of the tangent velocity component to zero [17]. The guides for the ANSYS/Fluent package recommend to pose only one condition at the output, i.e., for the pressure. Such boundary condition is natural in the case when the simulation uses experimental (clinical) data. Numerical calculations presented here demonstrate a good agreement of calculated results with experimental data. This is an argument for the application of the ANSYS/Fluent package widely used nowadays in hemodynamic computations [27].

The values $v_{\text{real}}, p_{\text{real}}^1, p_{\text{real}}^2$ were measured during the surgery [8, 20] and then filtered from noise and also smoothed. The method of measurement gives values of the velocity and pressure averaged over the cross-section. Figure 2 presents the graphs of dependence of the corresponding functions on time. Experimental data are approximately periodic. The preliminary calculations were performed for the time interval of 4 seconds and the analysis of the results had shown that two seconds are sufficient for stabilization of the state. Further calculations were performed within the two seconds interval.

The intravascular measurements of flow velocity and pressure in cerebral blood vessels near aneurysms at the modern state of medical equipment are possible, apparently, exclusively during the surgical intervention. The data the authors have got now are obtained during the operations for curing aneurysms before the stent installation. Measurements after stenting are planned and will be held in future. Calculating all the three states (before and after surgery and one year later) in this paper, we use the same values of velocity and pressure measured prior to stenting. Of course, this introduces certain errors in calculations which will be eliminated after obtaining necessary data.

Non-Newtonian blood properties are weakly expressed for the diameters of vessels and flow velocities considered in our calculations and hence we generally neglect them. It is shown in [16] that even for a slow blood flow inside the aneurysm bag between microcoils the consideration of non-Newtonian properties of blood is not determinative.

The stress–strain state of vessel walls is described with the use of a quasi-static approximation. At each time step (equal to 0.01 seconds) the fluid pressure on the vessel wall obtained in the hydrodynamic calculation is used as the boundary conditions in the calculation of the stationary stress–strain state of the vessel wall. The following model of an isotropic linear elastic material is used [18]:

$$\sum_{j=1}^3 \frac{\sigma_{ji}}{\partial x_j} = 0, \quad \Delta \sigma_{ij} + \frac{1}{1+\nu} \frac{\partial^2 (\sigma_{11} + \sigma_{22} + \sigma_{33})}{\partial x_i \partial x_j} = 0$$

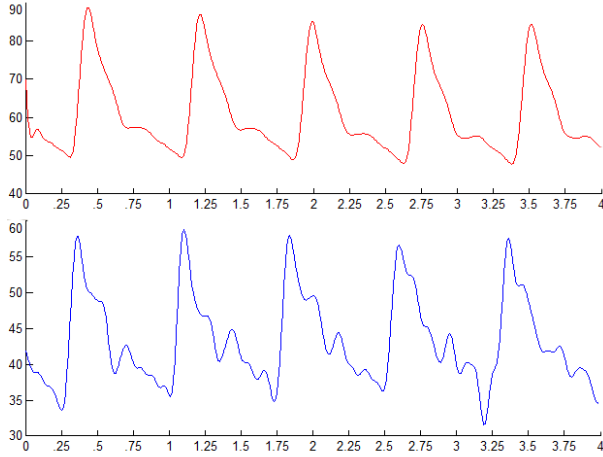


Figure 2. Clinical data, the pressure (top) and velocity (bottom).

where $\sigma = (\sigma_{ij})$ is the stress tensor, $i, j = 1, 2, 3$; ν is the Poisson coefficient. The first group of equations represents the equilibrium condition, the second group corresponds to the Beltrami–Michell relations. The pressure caused by the blood flow is given on the inner wall surface. The outer side of the wall is not loaded. The inlet and the et boundaries are strictly fixed.

The relation between the stress tensor (σ) and the strain tensor (ε) is determined by the Hooke law $\sigma = E\varepsilon$, where E is the Young modulus. This model is fairly common [6, 27].

The following parameters are taken for the wall of a normal (healthy) vessel: the wall thickness $h_c = 0.4$ mm, The Yung modulus $E = 1.0$ MPa, the Poisson coefficient $\nu = 0.49$. The zone of aneurysm has the parameters different from that of healthy vessel. The aneurysm wall thickness is $h_a = 0.1$ mm, $E = 1.2$ MPa, $\nu = 0.49$, which corresponds to experimental data [22].

The geometry of vessel walls and the aneurysm was constructed on the base of x-ray tomograms for all the three calculated cases. Using the ITK-SNAP code [30], we constructed three-dimensional representation of vessels in the anomaly area. The model of the stent used during the surgery is applied only for remodelling the shape of a vessel so that a coarse stent becomes a part of the wall after its deployment [3].

We use a tetrahedral calculation grid (see Fig. 1). Refining the grid of 56253 nodes and 233985 elements to the grid of 360570 nodes and 2036619 elements, i.e., 5 times, we obtain the deviation of less than 1% for the pressure, the absolute value of the velocity demonstrates slightly greater deviations (up to 5%). Further refinement of the grid does not practically affect the result, which demonstrates the adequacy of the grid used here.

Equations (1.1) were solved numerically by the SIMPLE method [21]. The spatial derivative is discretized with the use of the least squares method with values at centers of cells, the momentum is discretized by the second order upwind scheme.

The SIMPLE scheme has the first order of approximation in time.

The calculation of each configuration takes approximately 3 hours with the use of 4 computational kernels of the Intel Xeon E5540 processor.

2. Results. Hydrodynamic parameters

We calculate the following hydrodynamic parameters before the surgery, after it, and a year later: the flow velocity, streamline distribution, pressure, energy flux, shear stresses on the wall.

The results presented below were calculated for the time moment corresponding to systole, i.e., 380 ms from the beginning of the cardiac cycle. This time moment is interesting for quick changes in the velocity and pressure.

From the medical point of view, it is important to detect hazardous areas ('hot-spots') in the aneurysm and in the vessel near it. The question what parameter values determine these 'hot-spots' is not completely clarified. Based on the calculations, the pressure cannot be considered as such parameter because at each time moment its spatial distribution over the aneurysm and adjacent vessels is quite uniform (deviations are about 10%) which does not allow us to select any part of the vessel as a danger zone. The biggest difference between the maximal and the minimal pressure in the vessel in the whole time interval is approximately 45%. Figure 3 illustrates the spatial pressure distribution at the time moment when the distribution is maximally irregular.

2.1. Calculation of blood flow before the surgery

Figure 4a shows the velocity field streamlines in the vessel calculated before the surgery, the colour indicates the velocity value. Higher velocity values are observed in the subsidiary vessels, these are higher than 1 m/s, at the time moment shown in the figure the fluid flow having the maximal velocity almost completely fills the volume of the subsidiary vessels. Under normal conditions, velocity values about 1 m/s are observed only in the carotid artery, after that the velocity is decreased downstream due to the increase of the total cross section of the bloodstream [28]. In the place of bifurcation of the vessels the flow is pathologically twisted very much.

2.2. Calculations after the surgery

After stenting the flow velocity inside the aneurysm and in subsidiary vessels is reduced, which may be considered as a positive tendency in the case of a wide-neck aneurysm (see Fig. 4b). A decrease of blood flow velocity was also obtained in [11] in the case of the stent installation, which was considered as a positive result. The vortex insider the aneurysm is decreased and passes to an almost circular one, which is transformed into a cylindrical one in the cardiac cycle.

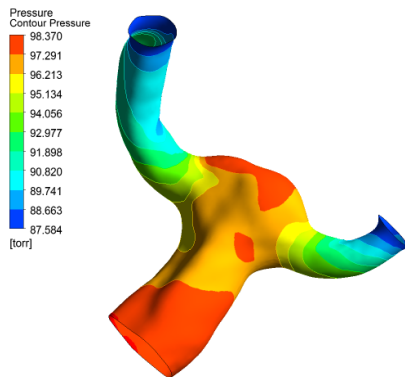


Figure 3. Pressure distribution in the vessel before the surgery.

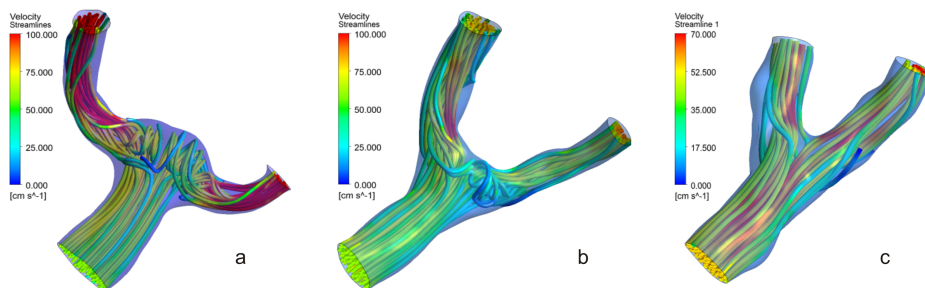


Figure 4. Streamlines in the vessel: before the surgery (a); after the surgery (b); a year later (c).

2.3. Checkup

One year after the surgery the geometry of vessels was noticeably changed, the span angle decreased, the intersection between the child branches almost disappeared, the geometry of the vessel in the neighbourhood of bifurcation was normalized. Zones of high velocities in the aneurysm and the child vessels were decreased, the vortex near the point of bifurcation disappeared (see Fig. 4c). Thus, the vessel had taken a geometrical configuration most conforming to a healthy one among all considered here. In this case we get the minimal velocity among the three configurations and there is practically no vorticity.

We also considered tee configurations before the surgery with inlet and outlet vessels artificially lengthened up to 10 diameters. These lengths were taken so that the velocity profiles could come to a stable state.

Test calculations with this geometric configuration show a qualitative and substantial quantitative agreement between the results for configurations with artificially lengthened inlet vessels and without them. In this connection, we mainly present the results of calculations for the configuration without lengthening the vessels.

3. Shear stress distribution on the vessel wall

At the moment there is no generally accepted criterion for determining the aneurysm rupture location. Apparently, the danger of rupture is affected by a combination of many factors. In particular, it is known [7] that increased shear stresses on the vessel wall lead to depletion and degradation of this wall, which can further contribute to the development of the aneurysm and to depletion of its walls, which leads to rupture. It is also assumed that small shear stresses lead to an insufficient metabolism in the wall and to formation of plaques [15].

The shear stresses on the vessel wall are determined by the formula [19]

$$\vec{\tau} = 2\mu\boldsymbol{\varepsilon} \cdot \vec{n}$$

where μ is the coefficient of dynamic viscosity, for blood it is equal to 0.004 kg/(m·s) [26], $\boldsymbol{\varepsilon}$ is the strain tensor, \vec{n} is the normal to the wall.

Below we present shear stress distributions on the wall calculated with the ANSYS/Fluent package. The shear stress distribution strongly depends on the position of the aneurysm on the vessel, of its form, and on the diameter of its neck. In this case the width of the incoming flow is close to the diameter of the cross-section of the aneurysm and hence we do not observe a local decrease of shear stress on the dome, the stresses are distributed uniformly over the dome.

It was shown in [19] that the values of shear stresses calculated with the use of the CFD package are greater than those measured with MRI. However, the qualitative difference is small. This fact may explain a sufficiently high mean value of shear stresses in our calculations. At the same time, this is an argument in favour of coincidence of high shear stress zones in our calculations and in the real vessel.

Before the surgery the maximal shear stresses are large and distributed over the vessel nonuniformly, they take the maximal values where the dome joins the branch vessels (see Fig. 5a).

After the surgery the shear stress distribution becomes more uniform and also decreases in value, which is a favourable indicator for further medical prognosis. A local increase of the shear stress appears where the blood comes to more narrow vessels (see Fig. 5b).

One year later the shear stress decreases and the maxima are concentrated at the point of bifurcation of vessels, which increases the risk of new aneurysm (see Fig. 5c).

Figure 6 shows the shear stresses before the surgery for the configuration with lengthened inlet and outlet vessels. Comparing this result with that for the configuration without vessel lengthening, we indicate their sufficiently good qualitative and quantitative coincidence.

4. Energy flux

There are several hypotheses for the optimal structure of a vascular network. One of such hypotheses is the minimality of the energy consumed for blood motion. In

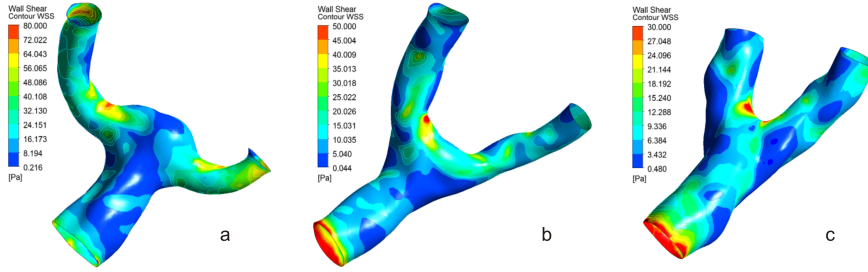


Figure 5. Shear stresses on the wall, before the surgery (a); after the surgery (b); a year later (c).

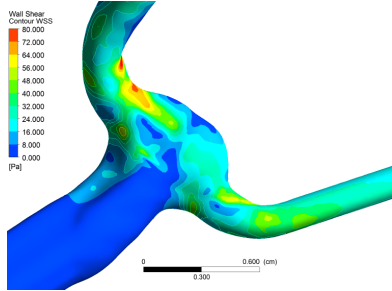


Figure 6. Shear stresses on the wall before the surgery for the configuration with lengthened inlet and outlet vessels.

this connection, it is interesting to compare the loss of energy flux for the three configurations considered here [8, 20].

The energy flux is calculated by the following formula:

$$\int_{\Sigma} \left(\frac{\rho |\mathbf{v}|^2}{2} + p \right) \cdot (\mathbf{v} \cdot \vec{n}) \, d\sigma$$

where Σ is the cross section of the vessel, \mathbf{v} is the velocity, p is the pressure, ρ is the density of blood, \vec{n} is the normal to the cross section of the vessel. The difference of energy fluxes before the anomaly and after it can be used to estimate the energy loss in the blood flow passage over the aneurysm.

Due to the optimal construction of blood circulation system, the energy loss in a blood flow through a vessel is sufficiently small. An aneurysm deforms the vessel wall and causes an increased energy loss in the flow. Before the surgery the energy loss in the flow passage through the tee was $\sim 9\%$, which is a sufficiently large value for the tee length approximately equal to 2 cm. After the surgery the geometry of vessels is reestablished up to a nearly healthy state with the flow energy loss of $\sim 4\%$. One year later the geometry of the vessel changes so that the energy loss becomes even less and equal to $\sim 1\%$ (see Fig. 7). Qualitatively similar changes in the energy flow are observed in calculations of configurations with lengthened vessels. This result shows that the anomaly is an energy-consuming formation in the vascular network and the organism must spend additional energy for blood flow motion in the presence of an anomaly.

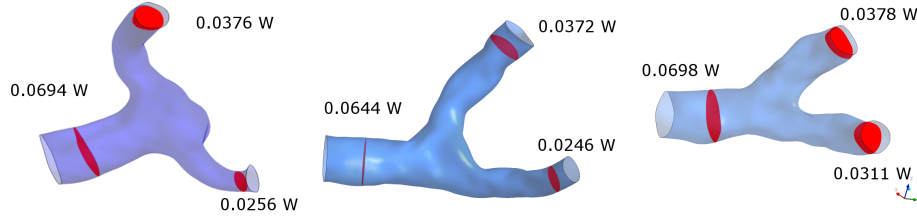


Figure 7. Energy flow.

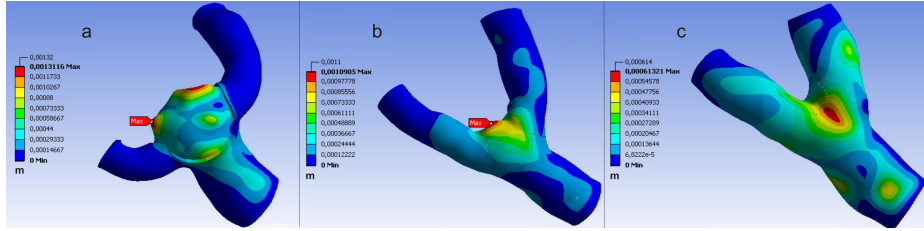


Figure 8. Displacements of the wall, (a) before the surgery, (b) after the surgery, (c) a year later.

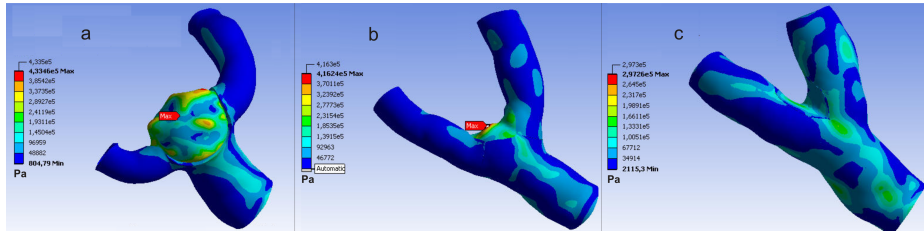


Figure 9. Von Mises stresses, (a) before the surgery, (b) after the surgery, (c) a year later.

5. Parameters of stressedly-deformed state of vessel walls

The calculation of wall deformation is performed relative to the initial (not loaded) state. The problem of the position of aneurysm rupture has no unique solution today [7], therefore, it is very important to calculate various parameters that may cause this rupture. Determining the location of the rupture, not only high hydrodynamic flow parameters, but also strength properties of the wall are important. One of possible criteria for destruction of the aneurysm wall is the von Mises criterion, its physical interpretation is that the von Mises stress characterizing the elastic strain energy attains its critical value [24]. The von Mises stress is calculated through the components of the stress tensor by the formula [14]:

$$\sigma_v = \left[\frac{1}{2} (\sigma_1 - \sigma_2)^2 + (\sigma_2 - \sigma_3)^2 + (\sigma_3 - \sigma_1)^2 \right]^{1/2}. \quad (5.1)$$

Stresses and displacements are calculated in the ANSYS/Mechanical package in the quasistatic model approximation of one-way hydroelasticity (1 way FSI).

5.1. Displacements and stresses before the surgery

Figures 8a, 9a present the distributions of displacements and von Mises stresses before the surgery, their isoline contours are very similar. The maxima of displacements and stresses are located at the dome of the aneurysm, but at different places. The places where the greatest stresses are concentrated are dangerous and just at these places the rupture of vessel wall may occur.

5.2. Displacements and stresses after the surgery

The stenting heavily changes the geometry of the vessel, and in comparison with the preoperative state the displacements are decreased by $\sim 17\%$, but the stresses by only $\sim 4\%$. After the stenting the qualitative difference between the location of displacement and the stress isolines increases (see Figs. 8b, 9b).

5.3. Displacements and stresses. Checkup

One year after the surgery the displacements and stresses had decreased almost 2 times in comparison with the previous results (see Figs. 8c, 9c). At the same time, their maxima were shifted from the dome of the aneurysm closer to the input vessel. Thus, the point of vessel bifurcation considered dangerous from the viewpoint of aneurysm rupture appeared to be unloaded, which can be interpreted as a good prognosis.

Aimed for comparative analysis, we carried out an additional stationary calculation of the hydro-elastic problem with time-averaged boundary conditions at the inlet and the outlets of the vessel. The maximal stresses and displacements in the stationary and unstationary calculations with separation of the aneurysm zone are always on the dome of the aneurysm and it is important that while these values are different in magnitude, they are geometrically located at the same positions, which allows us to apply quick calculations of ‘hot spots’ if necessary.

Unfortunately, obtaining experimental data characterizing the stress–strain state of the vessel *in vivo* is impossible now for ethical reasons because it requires significant intervention into the patient’s body which is not associated with medical indications.

6. Conclusion

The main features of this paper are nonstationary calculations of the actual aneurysm configuration and comparison of hydrodynamic flow parameters and strength properties of vessel walls before, after, and one year after the stenting. These results provide useful information for pre-surgical simulation and prognosis of dangerous points of the aneurysm.

The calculations performed in this research imply that immediately after the surgery the flow velocity in the aneurysm and child branches, shear stresses, energy loss when passing through the anomaly, von Mises stresses and wall displacements

are reduced, an almost circular vortex appears within the aneurysm. A year later the vessel takes such form that the vortex is completely absent and the flow velocity inside the vessel is minimal in comparison with other considered configurations. The surgery has significantly reduced the energy loss of blood flow in its passage through the tee and in a year the organism changes the geometry of the vessel so that the energy loss is $\sim 1\%$. There is a qualitative and largely quantitative coincidence of the results for the configurations with artificially lengthened supply vessels and without them.

In comparison with the results of [29] where the stationary case without separation of the zone of the aneurysm was considered, there is a qualitative agreement in the behaviour of streamlines, the distribution of pressure and shear stresses at the wall, but at the same time the quantitative values of the calculated parameters are significantly different.

References

1. *ANSYS FLUENT User's Guide*. ANSYS Inc.
2. *ANSYS FLUENT Theory Guide*. ANSYS Inc.
3. M. H. Babiker, L. F. Gonzalez, J. Ryan, F. Albuquerque, D. Collins, A. Elvikis, and D. H. Frakes, Influence of stent configuration on cerebral aneurysm fluid dynamics. *J. Biomech.* **45** (2012), No. 3, 440–447.
4. D. V. Bannikov, S. G. Chernyi, D. V. Chirkov, V. A. Skorospelov, and P. A. Turuk, Optimization design of the shape of hydraulic turbine flow part and flow analysis in it. *Vychisl. Tekhnol.* **15** (2010), 4 (in Russian).
5. S. De Bock, F. Iannaccone, G. De Santis, M. De Beule, P. Mortier, B. Verhegghe, and P. Segers, Our capricious vessels: The influence of stent design and vessel geometry on the mechanics of intracranial aneurysm stent deployment. *J. Biomech.* **45** (2012), No. 8, 1353–1359.
6. C. G. Caro, T. J. Pedley, R. C. Schroter, and W. A. Seed, *The Mechanics of the Circulation*. Oxford University Press, New York, 1978.
7. *Cerebral Aneurysm Surgery, Vols. I–III* (Ed. V. V. Krylov). Moscow, 2012 (in Russian).
8. A. P. Chupakhin, A. A. Cherevko, A. K. Khe, N. Y. Telegina, A. L. Krivoshapkin, K. Y. Orlov, V. A. Panarin, and V. I. Baranov, Measuring and analysis of local cerebral hemodynamics parameters of patients with cerebral vascular malformations. *J. Pathol. Blood Circ. Cardiosurgery* **4** (2012), 27–31.
9. C. Conca, F. Murat, and O. Pironneau, The Stokes and Navier-Stokes equation with boundary conditions involving the pressure. *Japan. J. Math. (N.S.)* **20** (1994), No. 2, 279–318.
10. B. J. Doyle, J. Killion, and A. Callanan, Use of the photoelastic method and finite element analysis in the assessment of wall strain in abdominal aortic aneurysm models. *J. Biomech.* **45** (2012), No. 10, 1759–1768.
11. G. Janiga, C. Rossl, M. Skalej, and D. Thevenin. Realistic virtual intracranial stenting and computational fluid dynamics for treatment analysis. *J. Biomech.* **46** (2013), 7–12.
12. J. H. Kim, T. J. Kang, and W. R. Yu, Mechanical modelling of self-expandable stent fabricated using braiding technology, *J. Biomech.* **41** (2008), No. 15, 3202–3212.
13. C. Kleinstreuer, Z. Li, and M. Farber, Fluid-structure interaction analyses of stented abdominal aortic aneurysms. *Ann. Review Biomed. Engrg.* **9** (2007), No. 1, 169–204.

14. A. E. H. Love, *Treatise On the Mathematical Theory of Elasticity*. Dover Publ., New York, 1934.
15. D. Ma, G. F. Dargush, S. K. Natarajan, E. I. Levy, A. H. Siddiqui, and H. Meng, Computer modelling of deployment and mechanical expansion of neurovascular flow diverter in patient-specific intracranial aneurysms. *J. Biomech.* **45** (2012), No. 13, 2256–2263.
16. H. G. Morales, I. Larrabide, A. J. Geers, M. L. Aguilar, and A. F. Frangi. Newtonian and non-Newtonian blood flow in coiled cerebral aneurysms. *J. Biomech.* **46** (2013), 2158–2164.
17. B. Muha and C. Canic, Existence of a weak solution to a nonlinear fluid-structure interaction problem modelling the flow of an incompressible, viscous fluid in a cylinder with deformable wall. *Arch. Rational Mech. Anal.* **207** (2013), 919–968.
18. V. V. Novozhilov, *Theory of Elasticity*. Sudpromgiz, 1958 (in Russian).
19. P. van Ooij, W. V. Potters, A. Guedon, J. J. Schneiders, H. A. Marquering, C. B. Majoie, E. van Bavel, and A. J. Nederveen, Wall shear stress estimated with phase contrast MRI in an in vitro and in vivo intracranial aneurysm. *J. Magnet. Resonance Imag.* **38** (2013), 876–884.
20. V. A. Panarin, K. Y. Orlov, A. L. Krivoschapkin, A. P. Chupakhin, A. A. Cherevko, A. K. Khe, N. Y. Telegina, and V. I. Baranov, An application of fluid dynamics computations in selecting for embolization scenario of cerebral arteriovenous malformation with a fistula component. *J. Pathol. Blood Circ. Cardiosurg.* **3** (2012), 39–43.
21. S. V. Patankar, *Numerical Heat Transfer and Fluid Flow*. Ch. 6, McGraw-Hill, New York, 1980.
22. T. J. Pedley, *The Fluid Mechanics of Large Blood Vessels*. Cambridge Univ. Press, Cambridge, 1980.
23. A. Quarteroni, M. Tuveri, and A. Veneziani. Computational vascular fluid dynamics: problems, models and methods. *Comput. Visual. Sci.* **2** (2000), 163–197.
24. Yu. N. Rabotnov, *Strength of Materials*. Fizmatlit, Moscow, 1962 (in Russian).
25. V. V. Ragulin, To the problem of viscous fluid flow through a bounded domain for a given gradient of pressure or head. In: *Continuous dynamics. Proc. Hydrodynamic Inst. Sib. Branch of USSR Acad. Sci.*, Issue 27, Novosibirsk, 1976, pp. 78–92.
26. R. F. Schmidt and G. Thews. *Human Physiology*. Springer Verlag, 1989.
27. D. M. Sforza, C. M. Putman, and J. R. Cebal, Hemodynamics of cerebral aneurysms. *Annu. Rev. Fluid. Mech.* **41** (2009), 91–107.
28. *Surgery of Cerebral Aneurysms*. (Ed. V. V. Krylov). Moscow, 2012 (in Russian).
29. N. A. Vorobtsova, A. A. Yanchenko, A. A. Cherevko, A. P. Chupakhin, A. L. Krivoschapkin, K. Yu. Orlov, V. A. Panarin, and V. I. Baranov, Modelling of cerebral aneurysm parameters under stent installation. *Russ. J. Numer. Anal. Math. Modelling.* **28** (2013), No. 5, 505–516.
30. P. A. Yushkevich, J. Piven, H. C. Hazlett, R. G. Smith, S. Ho, J. C. Gee, and G. Gerig, User-guided 3D active contour segmentation of anatomical structures: significantly improved efficiency and reliability. *Neuroimage* **31** (2006), No. 3, 1116–1128.